

Inhibitory Effect of Thymolphthalein for Carbon Steel Corrosion in Hydrochloric Acid Solution

H.M. Elabbasy¹, A. S. Fouda^{2,*}

¹ Misr higher Institute for Engineering and Technology, Mansoura, Egypt.

² Department chemistry, Faculty of Science, Mansoura University, Mansoura-35516, Egypt.

*E-mail: asfouda@hotmail.com,

Received: 12 December 2018 / *Accepted:* 21 January 2019 / *Published:* 10 March 2019

Thymolphthalein which is mainly used as chemical indicator, has been examined as corrosion inhibitor for carbon steel in 1 M hydrochloric acid solution. The examinations were performed by chemical techniques (weight loss) and many electrochemical techniques (Tafel, electrochemical impedance spectroscopy, electrochemical frequency modulation), in addition to surface analysis methods (scanning electron microscopy, energy dispersion spectroscopy). The output data indicated that Thymolphthalein adsorption on the metal surface fit well to Langmuir isotherm. Inhibition efficiencies were rising with Thymolphthalein concentration and reduced as temperature increases. The performance of the investigated compound, as obtained from the used techniques, ensures the truth of these techniques in the evaluation of this inhibitor.

Keywords: Thymolphthalein, Carbon steel, Adsorption, Langmuir isotherm, Hydrochloric acid

1. INTRODUCTION

Carbon steel (CS) is used greatly in pipelines to transfer liquids and gases, which results in the rust production. Although acids such as hydrochloric and sulphuric can be used in treatment process for removing that rust, this process leads to sharp corrosion. Many organic compounds that include N,S,P, and O in its structure were investigated widely for acidic corrosion of CS [1-9]. The studies prove that the inhibition influence of these compounds takes place by its adsorption on CS surface. That adsorption was found to be affected by metal surface charge, corrosive medium, and inhibitor structure [10-12]. The target of this investigation is evaluating of the inhibitory activity of Thymolphthalein for acidic CS corrosion.

2. EXPERIMENTAL METHOD

2.1. Material

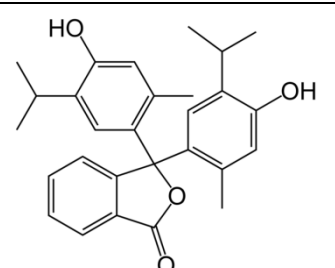
Current study is based on CS with the following composition as weight percentage: C = 0.200%, Mn = 0.350%, P = 0.024%, S = 0.003% and Fe = the remainder.

Corrosive solution was obtained from analytical grade 37% by its dilution with bidistilled water.

2.2. Investigated compound

Stock solution (10^{-3} M) of Thymolphthalein, which has the chemical structure shown in Table 1, was obtained using bidistilled water as solvent. The wanted concentrations (7×10^{-6} , 9×10^{-6} , 11×10^{-6} , 13×10^{-6} and 15×10^{-6} M) were prepared from that solution by dilution with bidistilled.

Table 1. Thymolphthalein chemical structure

Structure	IUPAC Name	Mol. Formula	Mol. wt, g/mol
	3,3-bis(4-hydroxy-2-methyl-5-propan-2-ylphenyl)-2-benzofuran-1-one	$C_{28}H_{30}O_4$	430.53

2.3. Weight loss (WL) tests

WL tests were carried out using six CS coupons with area 2.5 cm x 2 cm x 0.3 cm at temperatures from 25 to 50°C for 3 hrs. Emery papers from 320 to 1200 were used to prepare the coupons surface. Washing and cleaning the surface of the coupons were done using acetone and bidistilled water. The coupons weights were taken before and after immersion in corrosive solution without and with different concentrations of Thymolphthalein. WL at a definite time was taken. Surface coverage (θ) and inhibition efficiency (% IE) were determined using the following relation [13].

$$\% \text{ IE} = \theta \times 100 = [(W^\circ - W) / W^\circ] \times 100 \quad (1)$$

where W° is WL without Thymolphthalein and W is WL with Thymolphthalein.

2.4. Electrochemical methods

Gamry (PCI 300/4) instrument Potentiostat / Galvanostat/ZRA with a Gamry framework system established on ESA400, was used to complete electrochemical measurements. The instrument was connected to computer has E_{CHEM} analyst 5.58 to collect, plot, and fit data. The cell used in corrosion

process has three electrodes. The first one is SCE (used as reference electrode), the second one is a platinum electrode (used as auxiliary electrode), the last one is CS working electrode of 1 cm². All the given potentials were referred to SCE. In order to reach a steady state open circuit potential (E_{OCP}), CS electrode was left to stay in assay solution for 30 min. All the tests were occurred in aerated media at 25°C

Tafel tests were done at $E = E_{corr} \pm 250$ mV_{SCE}, at 0.5 mVs⁻¹ scan rate. Corrosion potential (E_{corr}) and corrosion current density (i_{corr}) were gotten from extrapolation of anodic and cathodic curves. Values of i_{corr} were used to calculate (θ) and (% IE) as follows [14]:

$$\% IE = \theta \times 100 = [1 - (i_{corr} / i_{corr}^0)] \times 100 \quad (2)$$

where i_{corr}^0 is corrosion current density without Thymolphthalein and i_{corr} is corrosion current density with Thymolphthalein.

Impedance tests were take place in the frequency extent (100 kHz and 0.1 Hz), by applying 5mV ac voltage peak-to-peak. %IE and θ of Thymolphthalein were obtained as follows:

$$\% IE = \theta \times 100 = [1 - R_{ct}^0 / R_{ct}] \times 100 \quad (3)$$

where R_{ct}^0 is the charge transfer resistance without Thymolphthalein and R_{ct} is the charge transfer resistance with Thymolphthalein.

2.5. Surface Analysis

CS surface was analyzed by energy dispersion spectroscopy (EDX) and scanning electron microscopy (SEM) techniques after exposure to corrosive solutions without and with Thymolphthalein for a period of 24 h. The examination was carried out by JOEL JSM-6510LV SEC.

3. RESULTS AND DISCUSSION

3.1. Weight Loss (WL) Tests

Curves of WL against time at 25°C for CS in 1 M HCl without and with many Thymolphthalein concentrations were demonstrated in Figure 1. It is clear that the blank curve is much higher than that with Thymolphthalein. The obtained linear relationships indicated absence of insoluble film during the corrosion procedure.

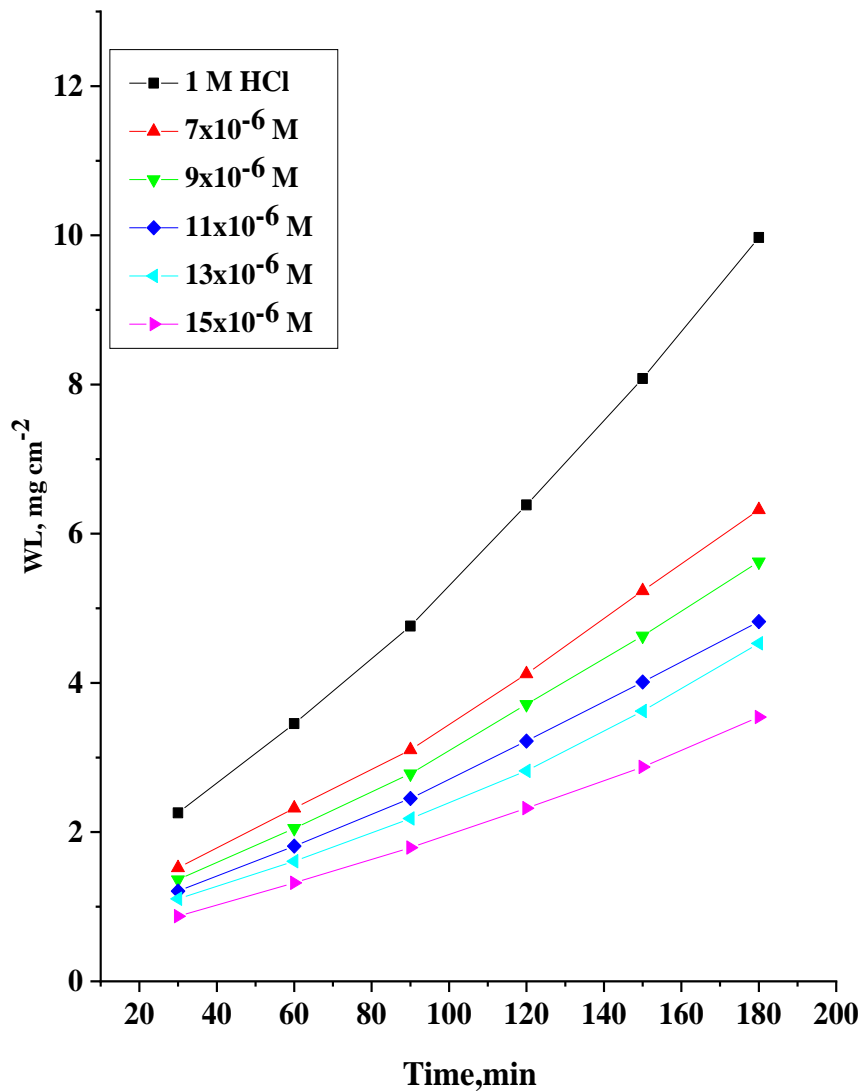


Figure 1. WL against time for CS in corrosive solution without and with Thymolphthalein at 25°C

3.2. Influence of Temperature

WL tests were used to prove the temperature influence on CS corrosion rate (k_{corr}) in corrosive solution. Figure 2 shows k_{corr} of CS in corrosive solution with many Thymolphthalein concentrations at different temperatures. % IE and Θ , which were calculated using equation (1), together with k_{corr} were putted in Table 2. As clear, k_{corr} rises with temperature while diminishes with Thymolphthalein concentration. Increasing of k_{corr} with increasing the temperature might be because when temperature increases, desorption of inhibitor from the metal surface increases [15]. Increasing the number of adsorbed molecules at CS surface was the reason of the increase of %IE with increasing Thymolphthalein concentration [16].

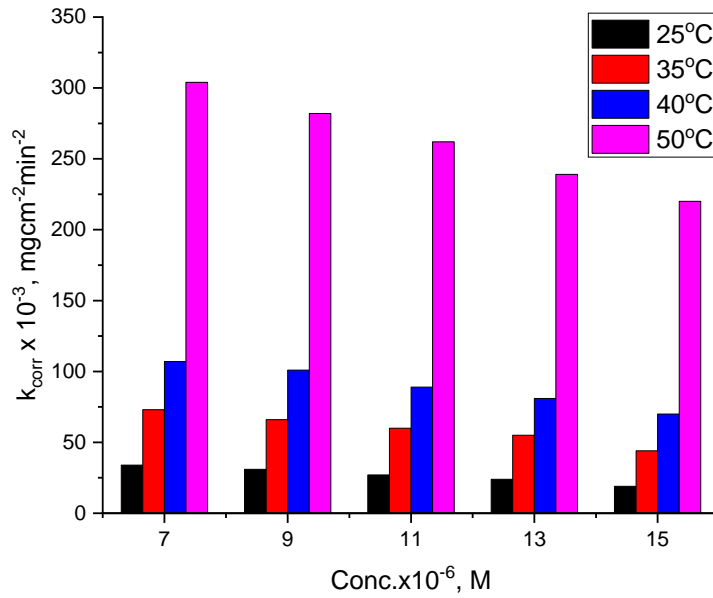


Figure 2. k_{corr} of CS in corrosive solution with many Thymolphthalein concentrations at different temperatures

Table 2. k_{corr} , θ and %IE at different Thymolphthalein concentrations for CS corrosion in corrosive solution

Temp., °C	25			35		
Conc., M	$k_{corr} \times 10^{-3}$, mg.cm ⁻² .min ⁻¹	θ	%IE	$k_{corr} \times 10^{-3}$, mg.cm ⁻² .min ⁻¹	θ	%IE
7×10^{-6}	34	0.355	35.5	73	0.241	24.1
9×10^{-6}	31	0.419	41.9	66	0.310	31.0
11×10^{-6}	27	0.496	49.6	60	0.372	37.2
13×10^{-6}	24	0.558	55.8	55	0.424	42.4
15×10^{-6}	19	0.645	64.5	44	0.537	53.7
Temp., °C	40			50		
Conc. (M)	$k_{corr} \times 10^{-3}$, mg.cm ⁻² .min ⁻¹	θ	%IE	$k_{corr} \times 10^{-3}$, mg.cm ⁻² .min ⁻¹	θ	%IE
7×10^{-6}	107	0.179	17.9	304	0.708	7.08
9×10^{-6}	101	0.225	22.5	282	0.135	13.5
11×10^{-6}	89	0.314	31.4	262	0.198	19.8
13×10^{-6}	81	0.377	37.7	239	0.269	26.9
15×10^{-6}	70	0.460	46.0	220	0.326	32.6

Activation energies for corrosion procedure (E_a^*) were gotten from Arrhenius relation as follows:

$$\log k_{corr} = \log A - (E_a^* / 2.303R) (1/T) \tag{4}$$

where A = constant, R= 8.314 joule/K.mol, and T = Kelvin temperature. Plots of log k_{corr} and 1000/T were illustrated in Figure 3. Enthalpy of activation for corrosion procedure (ΔH*) and entropy of activation for corrosion procedure (ΔS*) were determined by plotting log k_{corr}/T against 1/T (Figure 4), according to the following equation:

$$\log k_{\text{corr}}/T = \log (R/ Nh + \Delta S^*/ 2.303R) + (-\Delta H^*/ 2.303R) (1/ T) \tag{5}$$

where h = constant and N = number of Avogadro. Increasing of E^{*}_a and ΔH* with Thymolphthalein was because energy barrier that created in presence of Thymolphthalein. ΔH* values were found to have positive signs, indicating anodic dissolution reaction of CS. Negative ΔS* indicated that from reactants to the activated complex, the disorder decreased [17].

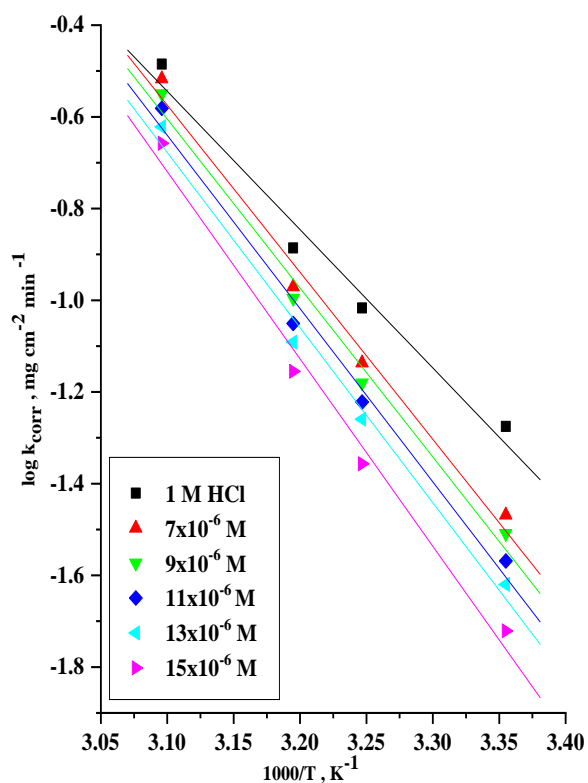


Figure 3. (log k_{corr}) against (1000/T) for CS in corrosive solution without and with many Thymolphthalein concentrations

Table 3. Parameters from activation process for CS in corrosive solution without and with many Thymolphthalein concentrations

Conc, M	E [*] _a , kJ mol ⁻¹	ΔH*, kJ mol ⁻¹	- ΔS*, J mol ⁻¹ K ⁻¹
corrosive solution	57.8	55.2	85.1
7 × 10 ⁻⁶	69.8	67.2	48.4
9 × 10 ⁻⁶	70.6	68.0	46.5
11 × 10 ⁻⁶	72.4	69.8	41.6
13 × 10 ⁻⁶	73.1	70.5	39.9
15 × 10 ⁻⁶	78.2	75.6	24.9

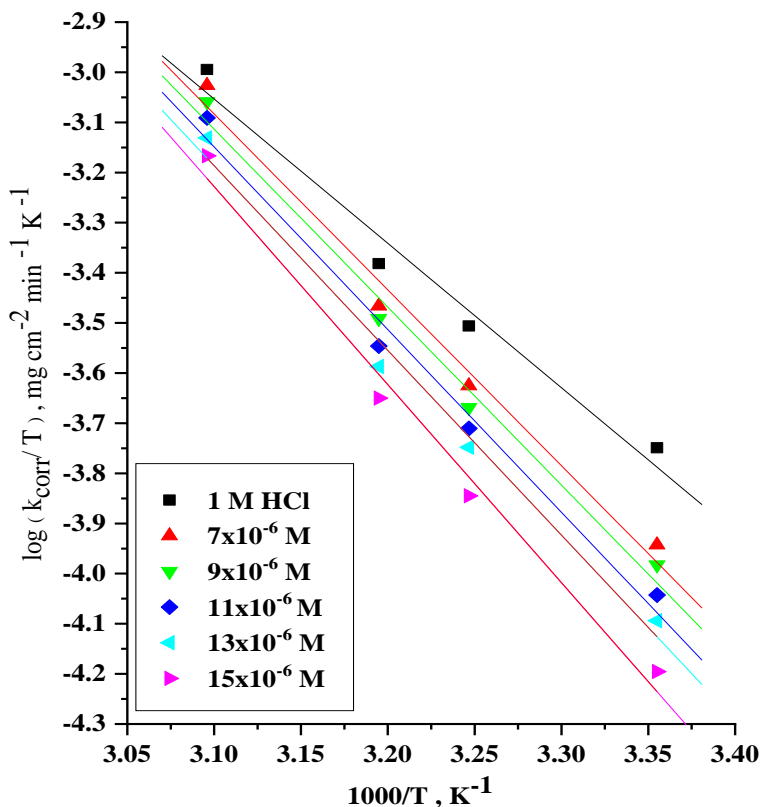


Figure 4. ($\log k_{\text{corr}}/T$) against $(1000/T)$ for CS in corrosive solution without and with many Thymolphthalein concentrations

3.3. Adsorption Process

Many adsorption isotherms were applied on the results, but the best one was Langmuir isotherm that specified as follows:

$$\theta/1-\theta = k_{\text{ads}} C \tag{6}$$

where k_{ads} is adsorption constant and C is Thymolphthalein concentration Figure 5 presents plots of $(\theta/1-\theta)$ against C at different temperatures. Adsorption free energy change ($\Delta G^{\circ}_{\text{ads}}$) were calculated as follows:

$$\log k_{\text{ads}} = \log(1/55.5) - (\Delta G^{\circ}_{\text{ads}}/2.303R)(1/T) \tag{7}$$

where $55. = [\text{water}]$ in solution. Adsorption enthalpy change ($\Delta H^{\circ}_{\text{ads}}$) was obtained from plotting $\log K_{\text{ads}}$ against $1/T$ (Figure 6) using the following relation [18]:

$$\log k_{\text{ads}} = (- \Delta H^{\circ}_{\text{ads}} / 2.303RT) + \text{constant} \tag{8}$$

Entropy changes of adsorption process ($\Delta S^{\circ}_{\text{ads}}$) were attained by applying the following equation [19]:

$$\Delta S^{\circ}_{\text{ads}} = (\Delta H^{\circ}_{\text{ads}} - \Delta G^{\circ}_{\text{ads}})/T \tag{9}$$

The gotten adsorption data were recorded in Table 4. Adsorption of Thymolphthalein on CS is a spontaneous because $\Delta G^{\circ}_{\text{ads}}$ have negative values [20, 21]. The tabulated $\Delta G^{\circ}_{\text{ads}}$ values were almost -40 kJ/mol, indicating the presence of physical and chemical adsorption (comprehensive adsorption), where covalent bond is formed through sharing charge of transferring it from the molecule to the metal

surface [22]. Negative ΔH°_{ads} indicated exothermic adsorption process [23]. Values of ΔS°_{ads} were negative as accompanied with exothermic adsorption process [24].

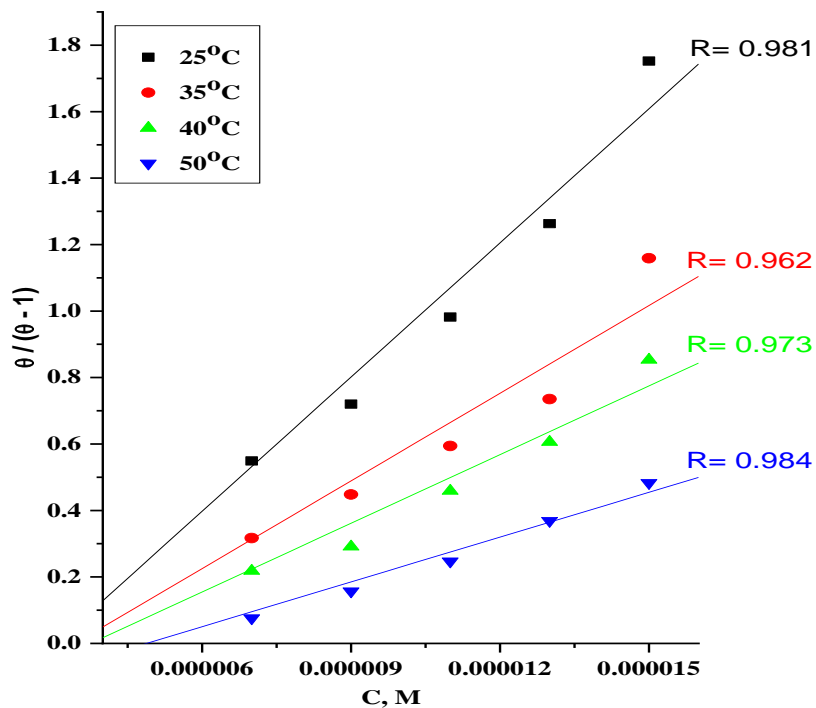


Figure 5. $(\theta/1-\theta)$ versus C at different temperatures for Thymolphthalein adsorption on CS surface in corrosive solution

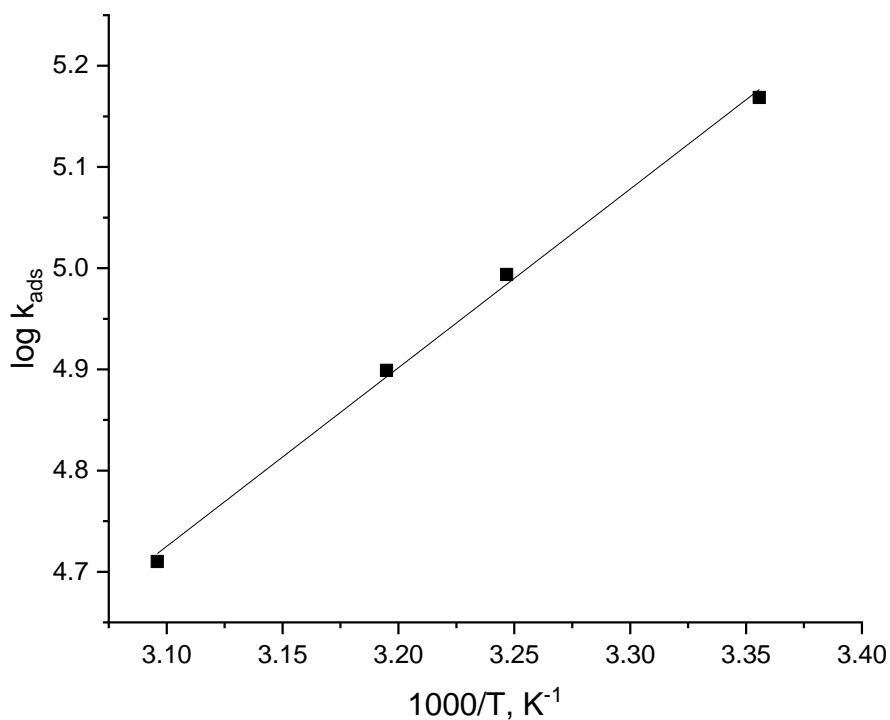


Figure 6. $\log k_{ads}$ against $1/T$ for CS in corrosive solution with Thymolphthalein

Table 4. Adsorption parameters for Thymolphthalein on CS in corrosive solution at different temperatures

Temp., °C	k_{ads}, M^{-1}	$-\Delta G^{\circ}_{ads}, kJ mol^{-1}$	$-\Delta H^{\circ}_{ads}, kJ mol^{-1}$	$\Delta S^{\circ}_{ads}, J mol^{-1} K^{-1}$
25	147450	39.4	33.8	18.9
35	98550	39.7		19.3
40	79250	39.8		19.2
50	51300	39.9		19.0

3.4. Potentiodynamic Polarization Tests

Figure 7 shows Tafel plots at 25°C for CS in corrosive solution without and with many Thymolphthalein concentrations. As indicated from the figure, increasing Thymolphthalein concentration leads to decrease cathodic "H₂ reduction" and anodic "metal dissolution" reactions. This behavior illustrated that a mixed type inhibitor mechanisms are present [25, 26]. %IE and θ from potentiodynamic polarization tests were calculated using equation (2). Table 5 shows the determined values of i_{corr} , E_{corr} , Tafel slopes (β_a and β_c), k_{corr} , θ and %IE. The data indicated that i_{corr} decreased with raising Thymolphthalein concentration and β_a & β_c remained almost unchanged with addition of Thymolphthalein, indicating that the adsorbed inhibitor decreases k_{corr} without affecting the reaction mechanism [27].

Table 5. i_{corr} , E_{corr} , β_c , β_a , k_{corr} , θ , and %IE for CS in the corrosive solution without and with many Thymolphthalein concentrations

Conc., M	$i_{corr}, mA cm^{-2}$	$-E_{corr}, mV vs SCE$	$\beta_c, mV dec^{-1}$	$\beta_a, mV dec^{-1}$	k_{corr}, mmy^{-1}	θ	% IE
corrosive solution	168	462	155	101	767.5	-----	-----
7×10^{-6}	142	519	156	136	650.6	0.155	15.5
9×10^{-6}	138	505	151	132	628.7	0.178	17.8
11×10^{-6}	119	501	131	121	542.7	0.291	29.1
13×10^{-6}	81.1	523	156	118	400.8	0.477	47.7
15×10^{-6}	77.8	525	145	129	355.6	0.536	53.6

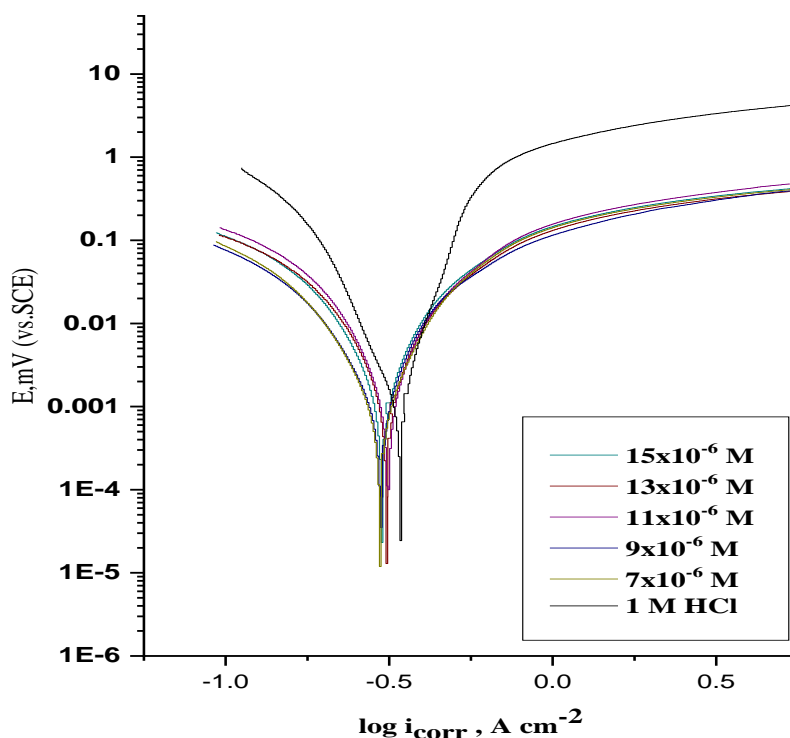


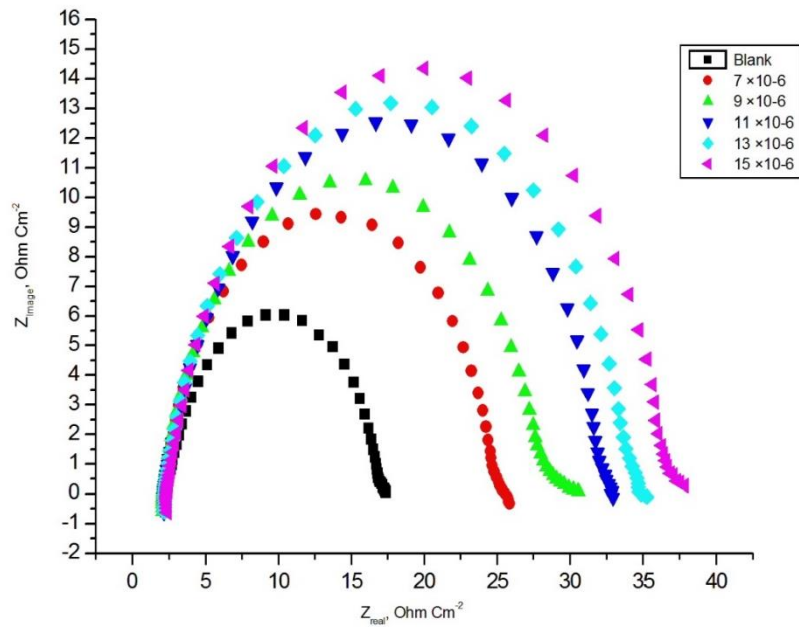
Figure 7. Potentiodynamic curves for CS in corrosive solution without and with many Thymolphthalein concentrations

3.5. Impedance Spectroscopy Tests (EIS)

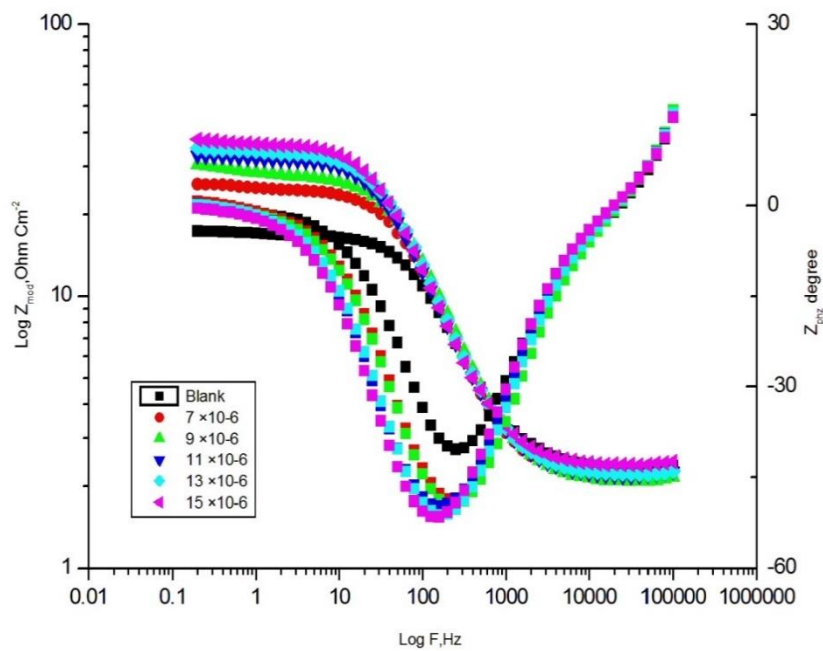
Nyquist plots (Figures 8 (a)) indicated that the presence of Thymolphthalein increased the semicircle diameter, which indicates an increase in metal corrosion resistance. The circuit shown in Figure 9 was used to fit EIS data. This circuit consists of the solution resistance (R_s) and the double layer capacitance (C_{dl}) (constant phase element) which parallel the charge transfer resistance (R_{ct}). R_s was at the high frequency and ($R_{ct}+R_s$) was at the low frequency in Bode plots (Figures 8 (b)). C_{dl} was determined as follows:

$$C_{dl} = 1 / (2\pi f_{max} R_{ct}) \quad (10)$$

where f_{max} is the higher frequency. Data from EIS for CS in corrosive solution without and with many Thymolphthalein concentrations was listed in Tables 6. As shown in the table, increasing Thymolphthalein concentration leads to increasing R_{ct} and decreasing C_{dl} , which indicates that the reduction of CS corrosion occurs through inhibitor adsorption at metal/acid [28,29].



(a) Nyquist plots



(b) Bode plots

Figure 8. Impedance plots for CS in the corrosive solution without and with many Thymolphthalein concentrations

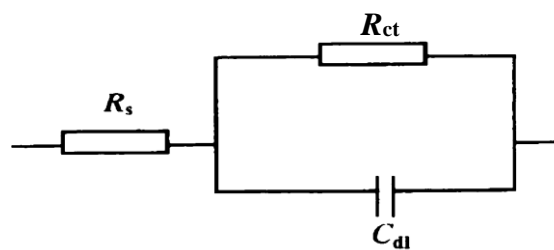


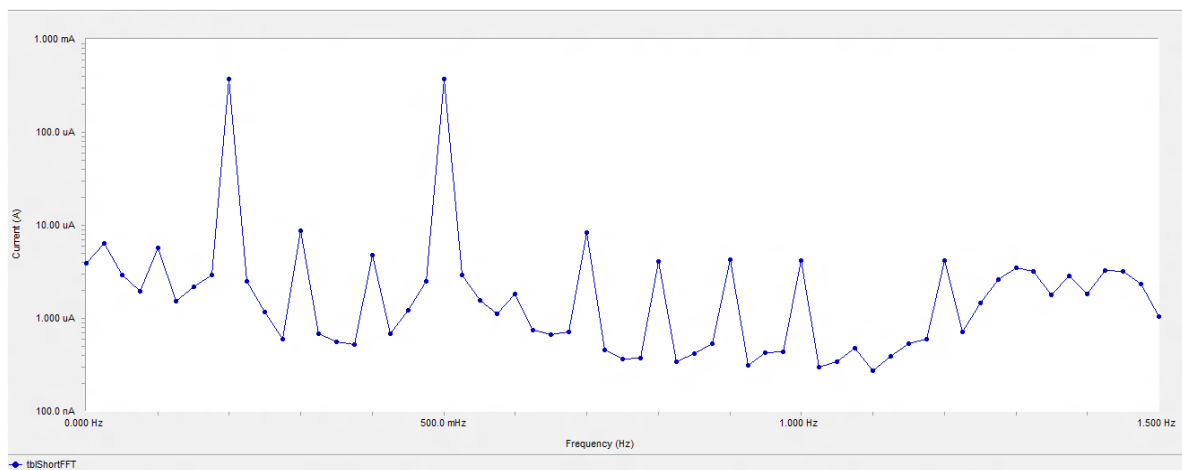
Figure 9. Circuit applied in fitting impedance data

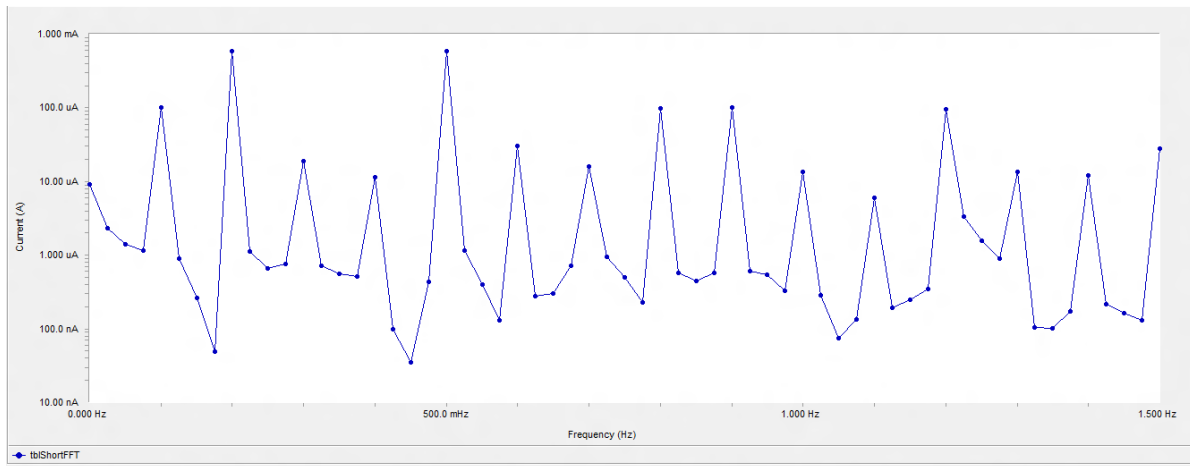
Table 6. Impedance data for CS in the corrosive solution without and with many Thymolphthalein concentrations

Conc., M	R_{ct} , $\Omega \text{ cm}^2$	C_{dl} , $\mu\text{F cm}^{-2}$	θ	% IE
corrosive solution	14.8	14.2	-----	-----
7×10^{-6}	22.9	13.0	0.354	35.4
9×10^{-6}	26.6	12.5	0.443	44.3
11×10^{-6}	30.5	8.1	0.523	52.3
13×10^{-6}	32.3	7.8	0.541	54.1
15×10^{-6}	34.6	7.3	0.572	57.2

3.6. Electrochemical Frequency Modulation (EFM) Tests

Figure 10(a,b) shows spectra for CS in corrosive solution and in presence of 15×10^{-6} M Thymolphthalein, respectively as obtained by EFM. EFM results (i_{corr} , β_c , β_a , causality factors (CF-2 & CF-3), k_{corr} , θ and %IE) were putted in Table 7. It was clear that as Thymolphthalein concentration increases, i_{corr} decreases and %IE increases. CF-2&CF-3 indicated that the results were of good quality. %IE resulted from chemical and electrochemical methods were almost in the same range as shown in Figure 11.

**(a)** Corrosive solution (1 M HCl)



(b) Corrosive solution + 15×10^{-6} M Thymolphthalein

Figure 10 (a,b). EFM spectra for CS in the corrosive solution without and with Thymolphthalein

Table 7. EFM results for CS in the corrosive solution without and with many Thymolphthalein concentrations

Conc., M	i_{corr} , mA cm ²	β_a , mVdec ⁻¹	β_c , mVdec ⁻¹	CF-2	CF-3	k_{corr} , mmy ⁻¹	Θ	IE %
Blank	598.7	97	113	1.93	3.21	273.5	----	----
7×10^{-6}	299.7	36	26	2.10	3.02	136.9	0.499	49.9
9×10^{-6}	282.3	33	34	2.37	2.62	129.0	0.528	52.8
11×10^{-6}	269.6	30	32	1.92	2.58	123.2	0.550	55.0
13×10^{-6}	257.6	28	30	2.16	3.07	117.7	0.570	57.0
15×10^{-6}	251.8	27	29	2.40	3.41	115.0	0.579	57.9

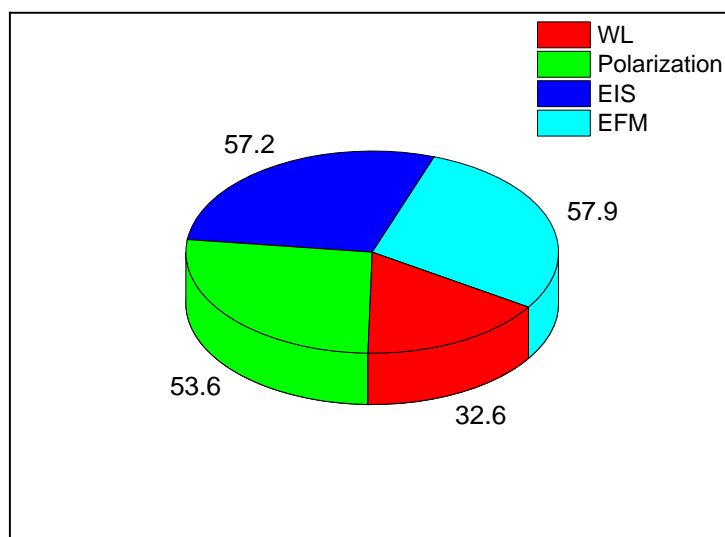


Figure 11. Comparison between % IE of 15×10^{-6} M of Thymolphthalein as obtained from the different techniques

3.7. Scanning electron microscopy (SEM)

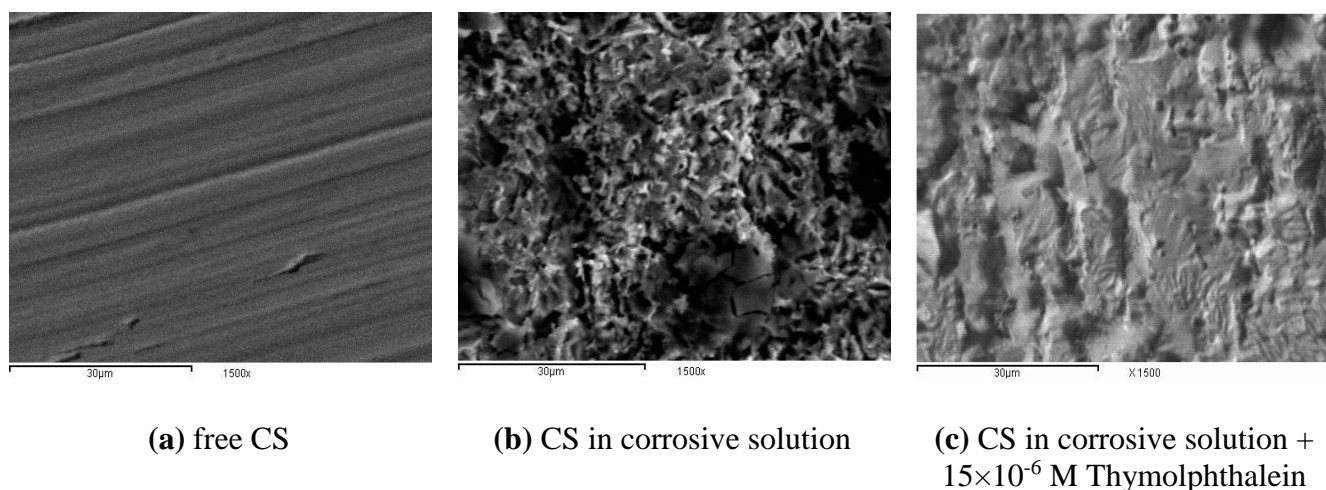


Figure 12(a-c) Different SEM micrographs of CS samples

Figure 12(a-c) shows different SEM micrographs of CS samples. Figure 12 (a) shows free CS. Figure 12(b) shows CS in corrosive solution. Figure 12(c) shows CS in corrosive solution + 15×10^{-6} M Thymolphthalein. Presence of CS in the acidic medium (Figure 12(b)) leads to increase of cracks and corrosion products on the surface. Presence of Thymolphthalein in the solution (Figure 12(c)) minimizes that cracks and corrosion products and makes the surface smoother. This might be due to formation of a passive layer through Thymolphthalein adsorption on the CS surface that blocks the active sites and minimizes metal contact with corrosive solution [31].

3.8. Energy Dispersion Spectroscopy (EDX) Analysis

By knowing the elements present on the metal surface using EDS, we can predict the effect of corrosive medium and inhibitor on the metal surface. Figure 13(a) displays free CS, Figure 13(b) displays CS surface in corrosive solution, while Figure 13(c) displays CS surface in corrosive solution + 15×10^{-6} M Thymolphthalein.

The analyzing details were presented in Table 8. The data indicated that there are C&O atoms on the free CS surface indicating presence of Fe_2O_3 layer on CS surface, while in addition of Thymolphthalein, additional lines appeared in Figure 13(c), that indicated presence of more C&O atoms because inhibitor adsorption on the surface.

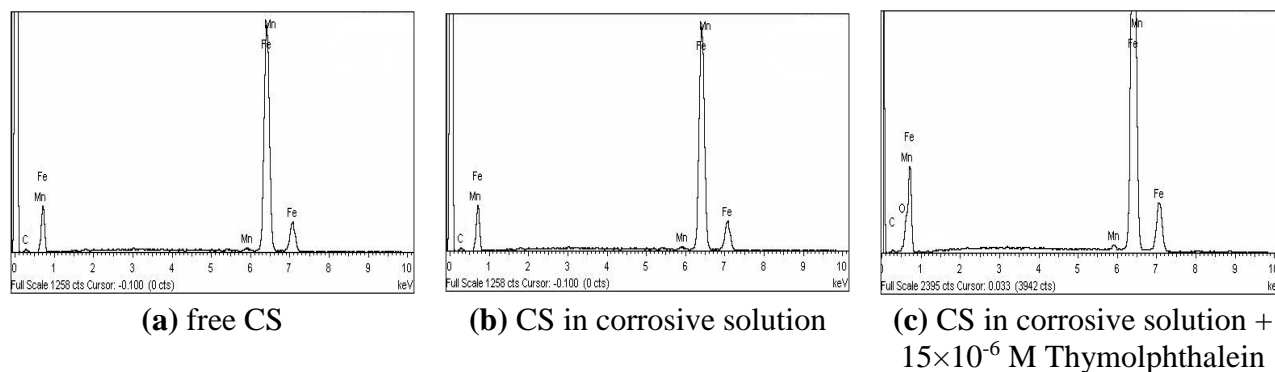


Figure 13(a-c) Micrographs of CS samples without and with Thymolphthalein

Table 8. Surface composition as weight percentage for CS after 3 days exposure to corrosive solution without and with Thymolphthalein

CS	Fe	Mn	C	O	Cl
free	95.43	0.63	3.94	---	---
in corrosive solution	65.45	0.57	3.32	30.15	0.51
in corrosive solution + 15×10^{-6} M Thymolphthalein	65.12	0.53	15.41	18.94	---

3.9. Corrosion Inhibition Mechanism

The inhibitory effect of Thymolphthalein on CS in corrosive solution may be attributed to the following reasons: i) O and S atoms which have free electron pairs, ii) aromatic rings which have $d\pi$ -electrons, iii) inhibitor molecular size, vi) heat of hydrogenation and v) interaction process between inhibitor and metal surface [32]. Since CS has the ability to form co-ordination bonds with O and S atoms [33], Thymolphthalein adsorption on CS surface can be referred to co-ordination with hetero atoms and aromatic rings π -electrons. Table 9 shows a comparison of some organic compounds used as inhibitors for CS in HCl medium. As shown from the table the compound used in this paper can be used as inhibitor for CS in HCl solution and it will be good inhibitor by increasing its concentration.

Table 9. Comparison between %IE of some organic compounds used as corrosion inhibitors for CS in 1 M HCl at 25°C

Compound	Conc., M	% IE	Reference
(Z)-N'-(1-(2-hydroxyphenyl) ethylidene)2-methylbenzohydrazide	15×10^{-6}	50.5	34
4-[9-(4-hydroxy-2-methyl-5-propan-2-yl-phenyl)-7,7-dioxo-8-oxa-7 λ 6-thiabicyclo [4.3.0] nona-1,3,5-trien-9-yl]-5-methyl-2-propan-2-yl-phenol (Thymol blue)	15×10^{-6}	83.5	35

Carbendazim(methyl2-benzimidazole carbamate	1×10^{-3}	89.6	36
1,5-Benzodiazepine derivative namely, 4Z-(2-Oxopropyl)-1,3-bis(prop-2-yn-1-yl)-2,3,4,5-tetrahydro-1,5-benzodiazepin-2-one (BZD-1)	1×10^{-6}	75.0	37
2-Amino-1,3,4-thiadiazole	17×10^{-6}	68.9	38
1-allyl- 1Hindole-2,3-dione	1×10^{-6}	74.9	39
3,3-bis(4-hydroxy-2-methyl- 5-propan-2-ylphenyl)- 2-benzofuran-1-one	15×10^{-6}	57.9	Our results

4. CONCLUSIONS

The efficiencies of Thymolphthalein on CS in corrosive solution solutions were studied by WL, potentiodynamic polarization, EIS, EFM, SEM, and EDS techniques. The summary of the results is as follows:

- 1- k_{corr} was increased by increasing temperature, indicates desorption of Thymolphthalein molecule was takes place by increasing temperature.
- 2- Thymolphthalein adsorption of on CS surface is physical and chemical.
- 2- By increasing Thymolphthalein concentration a more shifting in Tafel lines toward both positive and negative potentials take place, indicating a mixed type mechanism.
- 3- Increasing Thymolphthalein concentration decreases corrosion current density.
- 4- By adding more of Thymolphthalein, R_{ct} values increase while C_{dl} values decrease.
- 5- Presence of Thymolphthalein minimizes pits, cracks and corrosion products and makes the CS surface smoother.
- 6- The gravimetric and electrochemically results showed the similar range of IE.
- 7- All the obtained data indicated that the inhibitory effect of Thymolphthalein occurs through its adsorption on the CS surface.

References

1. A.S. Fouda, A.M. El-Desoky, D.M. Ead, *Int J Electrochem Sci.*, 8 (2013) 8823-8847
2. A.S. Fouda, A.A. Ibrahim, W.T. El-behairy, *Der Pharm. Chem.*, 6 (5) (2014) 144-157
3. A.S. Fouda, A. El-Bendary, M. Diab, A. Bakr, *J. Chem.*, 2 (2014) 302-319
4. A.S. Fouda, K. Shalabi, R. Ezzat, *J. Mater. Environ. Sci.*, 6 (4) (2015) 1022-1039.
5. M. Abdallah, H.M. Al-Tass, B.A. AL Jahdaly, A.S. Fouda, *J. Mol. Liq.*, 216 (2016) 590-597.
6. A.S. Fouda, M.A. Ismail, G.Y. EL-Ewady, A.S. Abousalem, *J. Mol. Liq.*, 240 (2017) 372-388.
7. M.A. Deyab, A.S. Fouda, M.M. Osman, S. Abdel-Fattah, *RSC Advances* 7 (71) (2017) 45232-45240.
8. A.S. Fouda, T. Fayed, M.A. Elmorsi, M. Elsayed, *J. Bio Tribo Corros.*, 3 (3) (2017) 33
9. M.A. Bedair, A.S. Fouda, M.A. Ismail, A. Mostafa, *Ionics*, (2018) 1-21
10. H. Zarrok, A. Zarrouk, R. Salghi, Y. Ramli, B. Hammouti, S.S. Al-Deyab, E.M. Essassi, H. Oudda, *Int. J. Electrochem. Sci.*, 7(9) (2012) 8958-8973.
11. H. Bendaha, A. Zarrouk, A. Aouniti, B. Hammouti, S. El Kadiri, R. Salghi, R. Touzan, *Phys. Chem.*

- News, 64 (2012) 95-103.
12. A. Zarrouk, B. Hammouti, H. Zarrok, R. Salghi, A. Dafali, L. Bazzi, L. Bammou, S.S. Al-Deyab, *Der Pharm. Chem.*, 4(1) (2012) 337-346.
 13. G.N. Mu, T.P. Zhao, M. Liu, T. Gu, *Corrosion*, 52 (1996) 853
 14. F. Bentiss, M. Lagrenee, M. Traisnel, *Corrosion*, 56 (2000) 733.
 15. F. Bentiss, M. Traisnel, N. Chaibi, B. Mernari, H. Vezin, M. Lagrenee, *Corros. Sci.*, 44(10) (2002) 2271-2289.
 16. M. Sahin, S. Bilgic and H. Ylmaz, *Appl. Surf. Sci.*, 195(1-4) (2002) 1-7.
 17. S.S. Afak, B. Duran, A. Yurt, G. Turkoglu, *Corros. Sci.*, 54 (2012) 251-259
 18. A. Popova, E. Sokolova, S. Raicheva and M. Christov, *Corros. Sci.*, 45 (2003) 33-58.
 19. I. Ahamad, R. Prasad, M.A. Quraishi, *Corros. Sci.*, 52 (2010) 1472-1481.
 20. A.A. El-Awady, B. Abd El-Nabey, S.G. Aziz, *Electrochem. Soc.*, 139 (1992) 2149-2154.
 21. A. Singh, R.S. Chaudhary, *Br. Corros. J.*, 31(4) (1996) 300-304.
 22. A. Yurt, S. Ulutas, H. Dal, *Appl. Surf. Sci.*, 253 (2006) 919-925.
 23. L. Tang, X. Lie, Y. Si, G. Mu, G. Liu, *Mater. Chem. Phys.*, 95 (2006) 29-38.
 24. X. Li and L. Tang, *Mater. Chem. Phys.*, 90 (2005) 286-297.
 25. J. Aljourani, K. Raeissi, M.A. Golozar, *Corros. Sci.*, 51 (2009) 1836.
 26. H. Amar, A. Tounsi, A. Makayssi, A. Derja, J. Benzakour, A. Outzourhit, *Corros. Sci.*, 49 (2007) 2936.
 27. T.P. Hoar, R.P. Khera, Proceedings 1st EuropSymp. on Corrosion Inhibitors, Ferrara, Italy, (1960) 73.
 28. M. Lagrenee, B. Mernari, M. Bouanis, M. Traisnel, F. Bentiss, *Corros. Sci.*, 44(3) (2002) 573-588.
 29. E. McCafferty, N. Hackerman, *J. Electrochem. Soc.*, 119(2) (1972) 146-154.
 30. X. Li, S. Deng, T. Li, *Electrochim. Acta.*, 54 (2009) 4089-4098.
 31. R.A. Prabhu, T.V. Venkatesha, A.V. Shanbhag, G.M. Kulkarni, R.G. Kalkhambkar, *Corros. Sci.*, 50 (2008) 3356-3362.
 32. M. Ehteshamzadeh, T. Shahrabi, M. Hosseini, *Anti-Corros. Meth. Mater.*, 53 (2006) 296-302.
 33. S. Sriram, R. Balasubramaniam, M. N. Mungole, S. Bharagava, R. G. Baligidad, *Corros. Sci.*, 48(5) (2006) 1059-1074.
 34. A.S. Fouda, K. Shalabi, A.E.El-Shennawi, R.M. Abo Shohba, A.A.El-Naggar, *International Journal of Innovative Research in Science, Engineering and Technology*, 3(3) (2014) 9876-9893.
 35. Ameena Mohsen Al-Bonayan, *Nature and Science*, 13(4) (2015) 106-115.
 36. I.M.Ali, M.I.Khan, *Int.J.Electrochem.Sci.*, 12 (2017) 2285.
 37. Y. El Aoufir, J. Sebhaoui, H. Lgaz, Y. El Bakri, A. Zarrouk, F. Bentiss, A. Guenbour, E.M. Essassi, H. Oudda, *JMES*, 8 (6) (2017) 2161-2173.
 38. A.S. Fouda, K. Shalabi, R. Ezzat, *J. Mater. Environ. Sci.*, 6 (4) (2015) 1022-1039.
 39. H. Zarrok, K. Al Mamari, A. Zarrouk, R. Salghi, B. Hammouti, S. S. Al-Deya5, E. M. Essassi, F. Bentiss, H. Oudda, *Int. J. Electrochem. Sci.*, 7 (2012) 10338 – 10357.